Burgers' turbulence with self-consistently evolved pressure

J. Fleischer and P. H. Diamond
Physics Department, University of California at San Diego, La Jolla, California 92093
(Received 4 March 1999; revised manuscript received 23 August 1999)

The Burgers' model of compressible fluid dynamics in one dimension is extended to include the effects of pressure back-reaction. The system consists of two coupled equations: Burgers' equation with a pressure gradient (essentially the one-dimensional Navier-Stokes equation) and an advection-diffusion equation for the pressure field. It presents a minimal model of both adiabatic gas dynamics and compressible magnetohydrodynamics. From the magnetic perspective, it is the *simplest* possible system which allows for ''Alfvenization,'' i.e., energy transfer between the fluid and magnetic field excitations. For the special case of equal fluid viscosity and (magnetic) diffusivity, the system is completely integrable, reducing to two decoupled Burgers' equations in the characteristic variables $v \pm v_{\mathrm{sound}}$ $(v \pm v_{\mathrm{Alfven}})$. For arbitrary diffusivities, renormalized perturbation theory is used to calculate the effective transport coefficients for forced ''Burgerlence.'' It is shown that energy equidissipation, not equipartition, is fundamental to the turbulent state. Both energy and dissipation are localized to shocklike structures, in which wave steepening is inhibited by small-scale forcing and by pressure back reaction. The spectral forms predicted by theory are confirmed by numerical simulations.

PACS number(s): 47.27.−i, 52.35.Ra, 41.20.Jb

I. INTRODUCTION

The challenge of understanding the puzzling phenomena generically dubbed ''intermittency'' has secured the status of turbulence as one of the premiere unsolved problem in classical physics. Intermittency phenomena complicate the simple and elegant picture of turbulence dynamics originally painted by Kol'mogorov. This model, which is a type of mean-field theory, is based upon assumptions of homogeneity, scale similarity, and unconstrained statistics governing the interaction between different degrees of freedom. Intermittency phenomena, however, *emphasize* the nontrivial structure of higher order (than quadratic) correlations by distorting the shape of the fluctuation probability distribution function (PDF), modifying spectra and introducing complex coherent effects into flow visualizations. Indeed, mounting evidence from numerous numerical and laboratory experiments suggest that spatiotemporally coherent structures are the cause of intermittency phenomena in turbulent flows. Such structures impose *precisely* the sorts of constraint on the phase dynamics of nonlinear interaction which is (arbitrarily) ignored in the Kol'mogorov paradigm. Thus the problem of understanding the formation and dynamics of structures in turbulence is a very popular research topic in nonlinear and statistical dynamics. A major obstacle to progress in this field is the resistance of the governing nonlinear PDE's to revealing nonperturbative solutions (even for simplied, limiting cases), from which insight into coherent structure properties and dynamics may be extracted. Hence, the recent flurry of studies of the Burgers' equation model of one-dimensional (compressible) turbulence is not at all surprising, since explicit, closed form solutions (resembling shock waves) to the unforced Burgers' equation have long been available. The more complicated case of stochastically forced ''Burgerlence'' is readily amenable to analysis by scaling and renormalization group methods. Of course, one-dimensional (1D) forced Burgerlence is also an attractive model for high-resolution numerical simulations. Thus, in spite of its oversimplicity and unphysical assumptions, Burgerlence retains its prominent position in turbulence models by virtue of its suitability as a ''laboratory animal'' for controlled experimentation in the application of theoretical methods to the description of turbulent flows.

In traditional Burgers' models, density or pressure changes result solely from changes in the velocity, much like the advection of a passive scalar. However, the evolution of these pressure terms suggest that they may grow enough to become dynamically significant. Indeed, the formation of shock waves and pancakelike density structures forces consideration of pressure back reactions on the fluid. Alternatively, the inclusion of pressure forces may be necessary from the very beginning, as in modeling pressure-induced flow or the basic magnetohydrodynamics (MHD) equations.

These considerations motivated us to extend the simple Burgers' model of turbulence to include the effects of an active pressure gradient. The pressure source, in turn, is coupled with the fluid through a convection-diffusion equation (e.g., adiabatic gas pressure and the continuity equation for density). For simplicity, we will consider the specific (yet representative) case of 1D compressible MHD, previously referred to as MHD Burgerlence [1]. While references to the other model systems will be given, where appropriate, the relative lack of attention given to MHD turbulence (compared with its neutral fluid counterpart) suggests that the most insightful interpretations may be in this field.

In this paper we present and analyze a 1D model of compressible, resistive MHD turbulence. In parallel, we interpret the model as a gas-dynamical system, with the magnetic field replaced by a gas density under the influence of an adiabatic pressure. We give an exact, closed form solution to the unforced system in the case of unity (magnetic) Prandtl number $\nu = \eta$. The solution represents shock waves in the characteristic variables of the dissipationless system. The scale invariance of inertial range Burgerlence is exploited to derive

coupled renormalization group (RG) recursion equations for the turbulenct viscosity (ν^t) and diffusivity (η^t) in the infrared limit, to one-loop order. This task is dramatically simplified by the observation that *Galilean invariance precludes renormalization of the interaction coupling coefficients*, as well as the purely advective coupling. For white-noise forcing, there is no amplitude (wave function) renormalization, leading to RG recursion equations for ν^t and η^t which closely resemble those for a (nonlinear) dynamical system in a 2D phase space. Of the three fixed points obtained, the one physical solution corresponds to a state of equidissipation (i.e., $\nu^t=\eta^t$; not equipartition, where $\langle\tilde{v}^2\rangle=\langle\tilde{B}^2\rangle$), *independent of the noise strengths* for $\tilde{v}$ and $\tilde{B}$!. (This conclusion still holds for spatially dependent noise.) The basin of attraction of the equidissipation fixed point encompasses all $\nu^t, \eta^t>0$. The RG exponents are determined by simple scaling relations and Galilean invariance constraints in the infrared limit. The scaling exponents and fixed point relations are then used to calculate ν^t and η^t, and thus $\langle\tilde{v}^2(k)\rangle$ and $\langle\tilde{B}^2(k)\rangle$, explicitly. As in the case of hydrodynamic Burgerlence, the forcing on small scales present in the white-noise spectra is strong enough to inhibit shock formation, i.e., the kinetic and compressional (magnetic) energy spectra scale as $E(k)\sim k^{-1}$, not k^{-2}. For spatially dependent noise, the amount of suppression depends on the correlation length of the forcing.

The remainder of this paper is organized as follows. In Sec. II, we present and discuss the pressure-coupled Burgers' model. Various properties of the model are elucidated. In Sec. III, we discuss dynamical aspects of the model. The unforced system is solved exactly for the case $\nu=\eta$. More general transport conditions (i.e., $\nu\neq\eta$) are discussed, and the forced model is introduced as a paradigm for more complicated turbulence systems. Next, the infrared statistical dynamics of forced MHD Burgerlence are analyzed using the direct-interaction approximation and RG methods for the case of uncorrelated white-noise sources (the extension to spatially dependent noise is treated in appendixes). Scaling arguments are used to determine the dynamical exponents. The one-loop RG recursion equations are used to obtain the physically relevant fixed point and its basin of attraction. Section IV contains a summary and discussion of results. Particular emphasis is given to the turbulent transport coefficients and the subsequent energy spectra. The implications of these results for other paradigms of MHD turbulence are discussed.

II. MODEL

Burgers' equation is the simplest nonlinear generalization of the diffusion equation. As a result, it appears as a first approximation in a variety of fields, including polymer motions [2], the growth of interfaces [3], and driven diffusion [4]. Burgers originally formulated the equation as a model of compressible fluid motion in one dimension [5], writing

$$\frac{Dv}{Dt}=\frac{\partial v}{\partial t}+v\frac{\partial v}{\partial x}=\nu\frac{\partial^2 v}{\partial x^2}, \tag{1}$$

where ν is the kinematic viscosity. It is the Navier-Stokes equation in one dimension, without the pressure gradient.

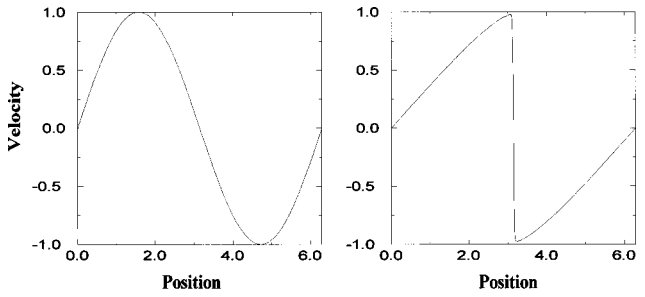

FIG. 1. Wave steepening in Burgers' equation. The initial sine wave on the left evolves to the steady-state sawtooth shock on the right.

The dynamics described by Eq. (1) are straightforward: convection steepens waves until they are balanced by viscosity (Fig. 1). Thus Burgers' equation captures the essential physics of shock formation [5] and frontogenesis [6,7]. It has also been used to model the 1D clumping of matter in an expanding universe (through the equation of continuity) [8,9].

In traditional models of Burgers' turbulence, density or pressure changes result solely from changes in the velocity, much like the advection of a passive scalar. However, the evolution of the neglected pressure term suggests that it may grow enough to become dynamically significant. Indeed, the formation of shock waves and pancakelike density structures forces consideration of pressure back reactions on the fluid. Alternatively, the inclusion of pressure forces may be necessary from the very beginning, as in modeling pressure-induced flow or the basic MHD equations. In the fluid case, the reintroduction of a pressure gradient effectively recovers the 1D Navier-Stokes equation. For the magnetic case, the inclusion of magnetic pressure creates a simplified model of the MHD equations. We will concentrate on the MHD system, and refer to the other models at the end. To simplify the physics, the derivations will be given for the force-free (i.e., decay) case. The addition of random forcing terms will be considered in later sections.

To begin, then, consider a fluid free to move in one direction (the $\hat{x}$ direction, say) with a perpendicular magnetic field ($\hat{z}$ direction) permeating it. The fluid behavior is described by the equations of continuity and momentum:

$$\frac{\partial\rho}{\partial t}+\frac{\partial(\rho v)}{\partial x}=0, \tag{2}$$

$$\frac{\partial v}{\partial t}+v\frac{\partial v}{\partial x}=-\frac{1}{\rho}\frac{\partial}{\partial x}\left[P(\rho)+\left(\frac{B^2}{8\pi}\right)\right]+\nu\frac{\partial^2 v}{\partial x^2}. \tag{3}$$

Here, an equation of state $P=P(\rho)$ has been implicitly assumed. The magnetic field evolves according to the diffusion equation

$$\frac{\partial\hat{B}}{\partial t}=\vec{\nabla}\times(\vec{v}\times\vec{B})+\eta\nabla^2\vec{B}, \tag{4}$$

which in one dimension reduces to

$$\frac{\partial B}{\partial t}=-\frac{\partial(vB)}{\partial x}+\eta\frac{\partial^2 B}{\partial x^2}. \tag{5}$$

In these equations, $\eta = c^2/4\pi\sigma$ is the magnetic diffusivity, and σ is the electrical conductivity of the fluid.

While Eqs. (2), (3), and (5) completely determine the system (with an appropriate equation of state), they are still too complicated for our purposes. To model the MHD behavior explicitly, assume that the fluid density changes on a length scale which is much longer than that of the magnetic field, i.e., $B^{-1}\partial_x B \gg \rho^{-1}\partial_x \rho$. In a perturbation expansion $\rho = \rho_0 + \rho_1(x) + \cdots$, only the lowest-order (constant) term would contribute. Alternatively, pressure balance could link density and magnetic fluctuations in a weakly compressible fluid, as in some parts of the solar wind plasma [10,11]. In this picture, Alfvenic properties are determined by magnetic variations on a constant density background. With this simplification, the model equations become

$$\frac{\partial v}{\partial t} + v\frac{\partial v}{\partial x} + B\frac{\partial B}{\partial x} = \nu\frac{\partial^2 v}{\partial x^2}, \tag{6}$$

$$\frac{\partial B}{\partial t} + \frac{\partial}{\partial x}(vB) = \eta\frac{\partial^2 B}{\partial x^2}, \tag{7}$$

where B has been normalized to represent the instantaneous Alfven velocity $B/\sqrt{4\pi\rho_0}$. Despite the approximations, Eqs. (6) and (7) still conserve energy (up to dissipation effects). Indeed, some straightforward manipulations give

$$\frac{\partial}{\partial t}\int \frac{1}{2}(v^2 + B^2)dx = -\int \left[\nu\left(\frac{\partial v}{\partial x}\right)^2 + \eta\left(\frac{\partial B}{\partial x}\right)^2\right]dx, \tag{8}$$

proving the assertion. The MHD Burgers model is thus the *simplest* possible set of equations which allow ''Alfvenization,'' i.e., the exchange of magnetic and fluid energies. The inclusion of compressional effects of the fluid density only complicates this basic picture, justifying *a posteriori* its neglect. The system represents a *meaningful*, if limited, model.

Equations (6) and (7) may also model the opposite limit of a fluid-dominated (i.e., unmagnetized) system. In this case, we allow arbitrary density variations and assume an adiabatic equation of state: $P = A\rho^\gamma$. Here A is a constant and $\gamma = C_p/C_v$ is the ratio of specific heats. Note that the Burgers' gas is certainly not adiabatic in the shock regions, but it is a reasonable approximation for the interstitial pressure. Since γ is also given by $(2+\delta)/\delta$, where δ is the number of dimensions, Eq. (7) now describes the gas momentum, where $B = \sqrt{3A\rho}$ is the local sound speed. Equation (6) is the continuity equation for the rescaled density with the addition of a diffusion term (consistent with a density-dependent gas pressure). Hence the MHD Burgers system has a broader applicability, and the transformations between these disparate models will prove useful in the analysis which follows.

The gas-dynamic viewpoint often provides insightful interpretations into the analogous MHD system. For example, the association between the gas density and the magnetic field highlights the latter's role as a compressive restoration force for the propagation of Alfven waves. Similarly, the global conservation (up to dissipation) of fluid momentum $\int(vB)dx$ corresponds to the conservation of magnetic flux. In the limit of negligible pressure back reaction, this conservation forces B to grow at shocks ($\dot{v} < 0$) and damp elsewhere. Recalling that the Burgers' system is energetically dominated by the shock regions, one sees that magnetic field amplification (there is no dynamo effect in one dimension) is intrinsically intermittent.

Another obvious gas-dynamic identity is the Galilean invariance of Eqs. (6) and (7). However, it is instructive to examine this symmetry in light of MHD and to review the transformation of the magnetic field from a fluid perspective. In our geometry, there is a magnetic field $\vec{B} = B\hat{z}$ with an induced electric field $\vec{E} = E\hat{y}$. Following a frame moving with velocity $\vec{v} = v\hat{x}$, the magnetic field may be written as

$$\frac{DB}{Dt} = \frac{\partial B}{\partial t} + v\frac{\partial B}{\partial x} \tag{9}$$

$$= \frac{\partial B}{\partial t} + v\left(-\frac{1}{c}\frac{\partial E}{dt}\right) \tag{10}$$

$$= \frac{\partial}{\partial t}\left(B - \frac{vE}{c}\right). \tag{11}$$

The partial derivative emphasizes that we are in a moving frame, prompting the definition of the transformed field $B' = B - vE/c$. Two comments are in order: (1) taking $\partial B'/\partial t = (\partial B'/\partial t')/(\partial t'/\partial t)$ gives the full relativistic transformation; and (2) $vE/c \sim (v/c)^2 B$, so $B' = B$ (i.e., Galilean invariance) to first order in v/c. Since MHD neglects the displacement current, both the magnetic and velocity fields are explicitly nonrelativistic. It is easily seen that the transformations $v'(x',t) = v(x-ut,t) + u$, $B'(x',t) = B(x-ut,t)$ leave Eqs. (6) and (7) invariant.

This symmetry is physically apparent in ideal MHD. Neglecting the viscous and forcing terms, the magnetic field is ''frozen'' into the fluid [12] [immediately evident by interpreting Eq. (6) as the continuity equation for ρ]. The Galilean invariance of the fluid then implies the invariance of the B field. However, the invariance argument does not depend on any spatial derivatives. Only the time derivative is needed to cancel the extra nonlinear term. Indeed, this cancellation highlights its relevance: Galilean invariance implies that the nonlinear coupling strength is unaffected (i.e. unrenormalized) by the following perturbative treatments [13]. It is useful to note that this symmetry applies in general to compressible, viscous MHD (in any number of dimensions).

III. DYNAMICS OF MHD BURGERLENCE

A. Unforced case

Since Eqs. (6) and (7) are generalizations of Burgers' equation, it is reasonable to wonder if the Burgers' shock dynamics are contained in the new system. Intuitively, we expect wave steepening to occur until it is balanced by pressure back reaction. A visualization of this dynamical evolution is shown in Fig. 2. Comparison with the *N*-wave structure of the original Burger's model (see Fig. 1) shows that shock formation is inhibited.

As a first step in the analytical characterization, suppose that the collisional transport rates of the two fields are equal; i.e., the (magnetic) Prandtl number $\mathrm{Pr} \equiv \nu/D = 1$. In terms of the characteristic, or Elsasser, variables $z_\pm = v \pm B$ the sys-

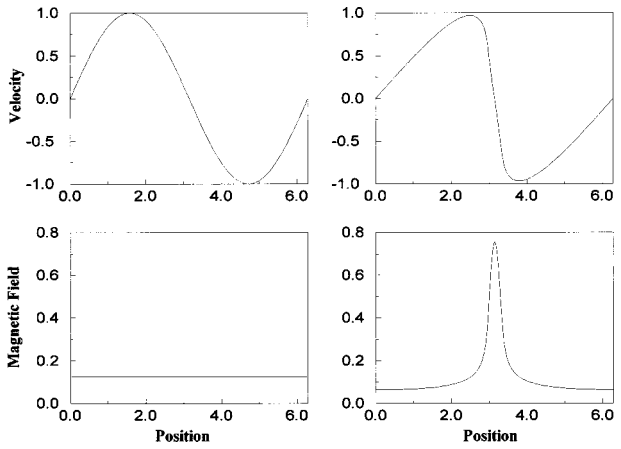

FIG. 2. Wave steepening in the MHD Burgers' model. The system evolves over the same period as for Fig. 1.

tem reduces to two decoupled Burgers' equations:

$$\frac{\partial z_{\pm}}{\partial t}+z_{\pm}\frac{\partial z_{\pm}}{\partial x}=\nu\frac{\partial^2 z_{\pm}}{\partial x^2}. \tag{12}$$

This reduction is not surprising, since in dissipationless MHD Burgerlence, initial value data is propagated along the characteristics $dx/dt=v\pm B$ at the constant characteristic velocity $v\pm B$. (In the gas-dynamic analogy, these variables just represent the combination of fluid and thermal speeds.) All the familiar results from Burgers' equation may be applied to this special case. In particular, the system can support Alfvenized shock waves, with regions of $\acute{z}_{\pm}<0$ steepening into fronts and $\acute{z}_{\pm}>0$ regions smoothing. This characteristic behavior implies that the MHD dynamics are controlled by the fluid velocity. Indeed, flux conservation requires magnetic concentration at the velocity shock fronts, while pressure back reaction acts to limit wave steepening. However, the relation $\partial_t(B_x)\approx -2(v_xB_x)$ implies that both negative and *positive* magnetic shocks are possible. Since these shocks dominate the energy spectrum of the system [14], magnetic intensity in MHD Burgerlence is intrinsically intermittent.

To examine the case $\nu\neq D$, it is useful to make the similarity transformations

$$v(x,t)=\left(\frac{\nu}{t}\right)^{1/2}f\left(\frac{x}{\sqrt{\nu t}}\right),\quad B(x,t)=\left(\frac{D}{t}\right)^{1/2}g\left(\frac{x}{\sqrt{\nu t}}\right) \tag{13}$$

so that Eqs. (6) and (7) become

$$-\tfrac{1}{2}f-\tfrac{1}{2}\zeta f'+ff'=gg'+Pf'', \tag{14}$$

$$-\tfrac{1}{2}g-\tfrac{1}{2}\zeta g'+(fg)'=Pg'', \tag{15}$$

where $P=Pr^{-1}=D/\nu$ and the prime refers to differentiation with respect to $\zeta\equiv x/\sqrt{\nu t}$. Integrating once gives

$$-\zeta f+f^2=-Pg^2+2Pf', \tag{16}$$

$$-\zeta g+2\,fg=2Pg'. \tag{17}$$

Now we can solve Eq. (17) for f, substitute into Eq. (16), and write $g(\zeta)=h(\zeta)^{-2/P}$ to obtain the single equation

$$4h''+Ph^{1-4/P}=\left(1+\frac{\zeta^2}{4}\right)h. \tag{18}$$

Equations of this type were studied by Thomas [15] and Herbst [16], who showed that the solvability condition is $P=1$. The solution, first given by Pinney [17], corresponds to the equal transport case discussed above.

The more general case of $\nu\neq D$ is not integrable, suggesting a more interesting interplay between the fluid and the pressure field. In particular, it raises the following question: how will arbitrary transport rates affect energy distribution and structure development?

B. Transport issues in steady-state Burgerlence

In contrast to the strictly *local* interactions of the Kol'mogorov paradigm for neutral fluids, interactions between *disparate scales* are fundamental to the dynamics of even the simplest incarnations of MHD turbulence. For example, the nonlocal interaction between a large-scale magnetic field and small-scale fluid motions (commonly referred to as the Alfven effect) inhibits and reduces eddy-eddy interaction and cascading. Thus in MHD turbulence the familiar Kol'mogorov inertial range spectrum $E(k)=\epsilon^{2/3}k^{-5/3}$ is replaced by the Kraichnan-Iroshnikov (KI) spectrum $E(k)=(\epsilon\tilde{v}_A)^{1/2}k^{-3/2}$, where $\tilde{v}_A^2=\langle\tilde{B}^2\rangle/4\pi\rho_0$. Indeed, the prominent footprint that large-scale magnetic patterns leave upon the inertial range physics of MHD turbulence, *even in the context of mean field (i.e., KI) theory*, suggests that *intermittency effects (induced by large-scale structures) will be at least as strong in MHD as in neutral fluid turbulence*. This suspicion is reinforced by consideration of the well-known reciprocal mechanisms whereby small-scale turbulence can induce and pump large-scale self-organization in MHD. The turbulent magnetic dynamo, which realizes the process of inverse transfer of magnetic helicity, is the classic example of such a mechanism. Asymmetries in the underlying turbulence are responsible for producing order on large scales. For example, a dynamo in 3D incompressible MHD occurs only if reflection symmetry of the turbulence is broken. Thus the dual reciprocal processes, whereby large-scale structures modulate MHD turbulence via the Alfven effect and whereby broken symmetry in the turbulence drives large-scale self-organization, together suggest self-reinforcing feedback in the dynamics of intermittency phenomena in MHD turbulence. The above discussion naturally concentrates the theorist's mind on several questions about the fundamental dynamics of intermittent pressure-dominated turbulence, which include (but are not limited to) the following.

(1) How much of the inertial range is affected by the direct interaction of disparate scales (e.g.,''Alfvenization'' in MHD)? Does equipartition occur between kinetic and compressional energies, and where? How does the energy distribution of the system vary with forcing? What roles do fluid and field really play in energy transfer and cascading, and in self-organization processes (i.e., dynamos)?

(2) Can the numerous''conceptual designs'' for structures in fluid and MHD turbulence, which abound in the literature

(e.g., flux tubes, fluid and magnetic vortices, etc.) be extracted from the governing nonlinear and dissipative PDE's Can useful closed form solutions which capture the physics of these concepts be found? How do these structures impact Alfvenization?

To explore these issues, we will introduce random noise sources to generate and sustain a turbulent steady-state. In the magnetic interpretation, the model equations become

$$\frac{\partial v}{\partial t}+v\frac{\partial v}{\partial x}+B\frac{\partial B}{\partial x}=\nu\frac{\partial^2 v}{\partial x^2}+\tilde{f}_v, \tag{19}$$

$$\frac{\partial B}{\partial t}+\frac{\partial}{\partial x}(vB)=D\frac{\partial^2 B}{\partial x^2}+\tilde{f}_B. \tag{20}$$

The presence of forcing highlights several dynamic regimes, depending on whether both fields, or just one, are randomly driven.

(1) $\tilde{f}_v\neq 0$, $\tilde{f}_B=0$: the fluid is actively stirred while B is advected. For low magnetic fields, pressure backreaction is negligible, and the system reduces to Burgers' advection of a passive scalar.

(2) $\tilde{f}_v=0$, $\tilde{f}_B\neq 0$: the magnetic field has an active source, and the fluid responds to the induced pressure. Obviously this is a B^2 (i.e., higher-order) effect.

(3) $\tilde{f}_v\neq 0$, $\tilde{f}_B\neq 0$: dual-drive turbulence.

The ''typical'' turbulence approach is case (1), where fluid forcing at large scales produces a Kol'mogorov-type energy cascade. In Burgers' turbulence, small-scale disturbances directly affect large-scale structures (through shocks), so forcing at all scales is the standard statistical tool. Hence we will treat the more general case of dual forcing first, discussing the other cases when appropriate.

C. Forced case

While the decay problem gives insight into the energy transfer between the fluid and the pressure field, it cannot model the transport properties of sustained (i.e., stationary) homogeneous turbulence. To treat this case, we introduced random forcing functions into the coupled Burgers' system. With these noise sources, the (magnetic) model is governed by

$$\frac{\partial v}{\partial t}+\lambda_v v\frac{\partial v}{\partial x}+\lambda_B B\frac{\partial B}{\partial x}=\nu\frac{\partial^2 v}{\partial x^2}+\tilde{f}_v, \tag{21}$$

$$\frac{\partial B}{\partial t}+\lambda_B\frac{\partial}{\partial x}(vB)=D\frac{\partial^2 B}{\partial x^2}+\tilde{f}_B. \tag{22}$$

Here, λ_v and λ_B are bookkeeping parameters which will eventually be set to unity. Their labeling is the most general one consistent with the conservation of energy.

While the random fluid forcing $\tilde{f}_v$ is introduced mainly as a turbulent energy source, $\tilde{f}_B$ has a variety of possible physical meanings. From a fluid perspective, $\tilde{f}_B$ represents seed pressure or temperature variations (as functions of the density), or the random ionization and dissociation and recombination of particles in a concentrated solution. From a cosmological perspective, $\tilde{f}_B$ models spontaneous density fluctuations, which are necessary for initial matter clumping. In the MHD interpretation, $\tilde{f}_B$ models random seeding of a perpendicular magnetic field, or fluctuations of an ambient force-free one.

Superficially, the presence of random forcing controls the dynamics of the system. However, this extended Burgers' model is a coupled system of two nonlinearly interacting fields, and the dynamical response to even simple sources is not *a priori* obvious. Indeed, these nonlinear interactions can induce non-Gaussian distributions, even for Gaussian noise. Physically, deviations from normality (i.e., intermittency effects) result from the development of shocks or other large-scale coherent structures. A flat initial spectrum allows these effects to be seen more clearly. To simplify the analysis, then, let us first assume that $\tilde{f}_v$ and $\tilde{f}_B$ are random white-noise forcing functions with no cross-correlations, i.e.,

$$\langle\tilde{f}_i(k,\omega)\tilde{f}_j(k',\omega')\rangle=S_i\delta_{ij}\delta(k-k')\,\delta(\omega-\omega'), \tag{23}$$

where $i,j\in\{v,B\}$. Note that the forcing is now distributed equally on all spatial scales. (The extension to spatially-dependent noise is treated in Appendix B.) An example of the forced dynamics is shown in Fig. 3.

For convenience, we will call the range of dynamic response the inertial range. Technically, though, we are considering a regime of driven turbulence, rather than a proper ''inertial'' range (i.e., a momentum-dominated response to purely large-scale forcing). The only difference is the bandwidth of the noise sources, but the corresponding interpretations differ significantly. A reconciliation between these two viewpoints will follow the analysis, where the results will allow a basis for comparison.

1. Scaling arguments

We are interested in fully developed MHD Burgerlence for long times and large distances. For homogeneous turbulence in the inertial range, there are no intrinsic scale lengths. Dynamical terms will dominate beyond the dissipative lengths, and correlation functions will asymptotically approach simple algebraic forms [18,19]. For example, the velocity autocorrelation $\langle\delta v^2(\delta x,t)\rangle$ will have the homogeneous form $(\delta x)^{-\alpha}\langle\delta v^2(t/\delta x^a)\rangle$. Alternatively, $\omega\propto k^a$ provides a nonlinear dispersion relation for the system [20].

To see the dependence of the various parameters on the scale size, suppose that we change the length scale $x\to bx$. Under this similarity transformation, the other variables will scale, in general, as $t\to b^a t$, $v\to b^c v$, and $B\to b^d B$. After this rescaling, Eqs. (21) and (22) become

$$\frac{\partial v}{\partial t}+\lambda_v b^{a+c-1}v\frac{\partial v}{\partial x}+\lambda_B b^{a-c+2d-1}B\frac{\partial B}{\partial x}=\nu b^{a-2}\frac{\partial^2 v}{\partial x^2}+b^{a-c}\tilde{f}_v, \tag{24}$$

$$\frac{\partial B}{\partial t}+\lambda_B b^{a+c-1}\frac{\partial(vB)}{\partial x}=Db^{a-2}\frac{\partial^2 v}{\partial x^2}+b^{a-d}\tilde{f}_B, \tag{25}$$

Consistent scaling of λ_B implies that $c=d$. Therefore, v and B scale the same way (necessary for the local conservation of

energy). The assumption of white noise implies that $\langle \tilde{f}^2 \rangle = \int \tilde{f}^2 dk\, d\omega$ is invariant to a change in scale. Hence, $a = 2c+1$; there is only one independent exponent to find.

Choosing a as the necessary exponent, the parameters (i.e., coefficients) of Eqs. (24) and (25) now scale as

$$\begin{Bmatrix} \lambda_v \\ \lambda_B \end{Bmatrix} \to b^{3(a-1)/2} \begin{Bmatrix} \lambda_v \\ \lambda_B \end{Bmatrix}, \quad \begin{Bmatrix} \nu \\ D \end{Bmatrix} \to b^{a-2} \begin{Bmatrix} \nu \\ D \end{Bmatrix}. \tag{26}$$

Finding a is equivalent to finding the transport behavior of the system. This is immediately apparent from the relation $x^a \sim t$. For example, $a=2$ signifies diffusion, as in the similarity transformation used in Eqs. (13). That diffusive assumption was motivated by the Hopf-Cole solution to the *unforced* Burgers' system. In the case here, the presence of forcing *dynamically alters* the system response, modifying the transport relationship.

It is critically important to note that random Galilean invariance implies that the coupling coefficient λ is unaffected by the the nonlinear interactions (i.e., no vertex corrections) [13]. This is seen most easily from Burgers' equation (12), with $z_\pm$ acting as velocity. In a moving reference frame, $z_\pm(x,t) \to z_\pm(x - \lambda_z z_\pm t, t)$. Note that the coupling coefficient is necessary in the velocity boost, since the first-order correction (i.e., symmetry generator) is nonlinear. Galilean invariance and scale invariance can be preserved only if λ_z is unrenormalized. By the arguments in Sec. III B, this condition also holds for both λ_v and λ_B. This constraint immediately gives the scaling exponents $a=1$ and $c=0$. That is, $x \sim t$, so transport is ballistic rather than diffusive. The *speed* of propagation, though, can only be determined through approximation methods.

2. Direct-interaction approximation

The direct-interaction approximation treats the nonlinearites of Eqs. (21) and (22) as perturbations. The scaling behavior is then determined by spatially averaging over the interacting modes. To this end, we Fourier transform the system in space and time, giving

$$(-i\omega + \nu k^2) v_{k,\omega} = -\lambda_v \left\langle v \frac{\partial v}{\partial x} \right\rangle_{k,\omega} - \lambda_B \left\langle B \frac{\partial B}{\partial x} \right\rangle_{k,\omega} + \tilde{f}_v, \tag{27}$$

$$(-i\omega + Dk^2) B_{k,\omega} = -\lambda_B \left\langle \frac{\partial}{\partial x}(vB) \right\rangle_{k,\omega} + \tilde{f}_B, \tag{28}$$

where the angular brackets $\langle \cdots \rangle_{k,\omega}$ represent a convolution. These equations may be solved perturbatively by an expansion in the nonlinear interaction strengths $\lambda_v \sim \lambda_B$:

$$\begin{aligned} v_{k,\omega} &= v^{(0)}_{k,\omega} + \lambda_v v^{(1)}_{k,\omega} + \lambda_v^2 v^{(2)}_{k,\omega} + \cdots, \\ B_{k,\omega} &= B^{(0)}_{k,\omega} + \lambda_B B^{(1)}_{k,\omega} + \lambda_B^2 B^{(2)}_{k,\omega} + \cdots. \end{aligned} \tag{29}$$

The linear behavior is a simple diffusive response to the forcing, where the bare (unrenormalized) propagators are defined by $G_v^0 \equiv (-i\omega + \nu k^2)^{-1}$ and $G_B^0 \equiv (-i\omega + Dk^2)^{-1}$. Note the implicit assumption that convection is dominated by forcing. The nonlinear effects appear as first-order corrections:

$$\begin{aligned} v^{(1)}_{k,\omega} = -ikG_0^v(k,\omega) \sum_{k',\omega'} [&\lambda_v v^{(0)}_{k',\omega'} v^{(0)}_{k-k',\omega-\omega'} \\ &+ \lambda_B B^{(0)}_{k',\omega'} B^{(0)}_{k-k',\omega-\omega'}], \end{aligned} \tag{30}$$

$$\begin{aligned} B^{(1)}_{k,\omega} = -ik\lambda_B G_0^B(k,\omega) \sum_{k',\omega'} [&v^{(0)}_{k',\omega'} B^{(0)}_{k-k',\omega-\omega'} \\ &+ B^{(0)}_{k',\omega'} v^{(0)}_{k-k',\omega-\omega'}]. \end{aligned} \tag{31}$$

These terms appear recursively in the second-order perturbations

$$\begin{aligned} (-i\omega + \nu k^2) v^{(2)}_{k,\omega} = -ik \sum_{k',\omega'} [&\lambda_v v^{(0)}_{-k',-\omega'} v^{(1)}_{k+k',\omega+\omega'} \\ &+ \lambda_B B^{(0)}_{-k',-\omega'} B^{(1)}_{k+k',\omega+\omega'}], \end{aligned} \tag{32}$$

$$\begin{aligned} (-i\omega + Dk^2) B^{(2)}_{k,\omega} = -ik\lambda_B \sum_{k',\omega'} [&v^{(0)}_{-k',-\omega'} B^{(1)}_{k+k',\omega+\omega'} \\ &+ B^{(0)}_{-k',-\omega'} v^{(1)}_{k+k',\omega+\omega'}]. \end{aligned} \tag{33}$$

Equations (32) and (33) define renormalized propagators, or (equivalently) effective transport coefficients. In the hydrodynamic limit $(k,\omega \to 0)$, these coefficients become

$$\begin{aligned} \nu^t = \frac{1}{4\pi^2} \int dk'\, d\omega' [&\lambda_v^2 G_0^v(k',\omega') |v^{(0)}_{k',\omega'}|^2 \\ &+ \lambda_B^2 G_0^B(k',\omega') |B^{(0)}_{k',\omega'}|^2], \end{aligned} \tag{34}$$

$$\begin{aligned} D^t = \frac{\lambda_B^2}{8\pi^2} \int dk'\, d\omega' [&G_0^B(k',\omega') |v^{(0)}_{k',\omega'}|^2 \\ &+ G_0^v(k',\omega') |B^{(0)}_{k',\omega'}|^2], \end{aligned} \tag{35}$$

using the continuum approximation $\Sigma_{k',\omega'} \to \int [dk'\, d\omega'/(2\pi)^2]$. Integrating over ω' gives

$$\nu^t = \frac{1}{4\pi} \left[\frac{\lambda_v S_v}{\nu^2} + \frac{\lambda_B S_B}{D^2} \right] \int_{k_{\min}}^{\infty} \frac{dk'}{k'^4}, \tag{36}$$

$$D^t = \frac{\lambda_B^2}{2\pi(D+\nu)} \left[\frac{S_v}{\nu} + \frac{S_B}{D} \right] \int_{k_{\min}}^{\infty} \frac{dk'}{k'^4}. \tag{37}$$

Here S_v and S_B are the (white) noise strengths of the forcing functions [see Eq. (23)]. Note that the interaction of slow modes causes the transport coefficients to diverge. Finally, performing the spatial average gives

$$\nu^t = \frac{1}{12\pi k_{\min}^3} \left[\frac{\lambda_v S_v}{\nu^2} + \frac{\lambda_B S_B}{D^2} \right], \tag{38}$$

$$D^t = \frac{1}{6\pi k_{\min}^3} \left[\left(\frac{\lambda_B^2}{\nu + D} \right) \left(\frac{S_v}{\nu} + \frac{S_B}{D} \right) \right]. \tag{39}$$

Since we are in the inertial range, these turbulent diffusivities will dominate the original bare ones. Letting $\nu \to \nu^t$ and $D \to D^t$, Eqs. (38) and (39) become self-consistent recursion relations for the effective viscosity and diffusivity. Carrying out the algebra, one finds that

$$D^t = \nu^t \left[\frac{\lambda_v^2 S_v S_B - \alpha S_B (\nu^t)^3}{\alpha (2S_v - S_B)(\nu^t)^3 - \lambda_v^2 S_v^2} \right], \tag{40}$$

where $\alpha = 6\pi k_{\min}^3$. Using this relationship, the turbulent diffusivity is determined by the equation

$$x^3 - \frac{b}{2}[5dc - (2c-1)^2]x^2 + abc[2(c+d)-1]x - \frac{a^2 bc}{2}(c+d) = 0, \tag{41}$$

where $x = \alpha(\nu^t)^3$, $a = \lambda_v^2 S_v$, $b = \lambda_B^2 S_B$, $c = S_v/S_B$, and $d = \lambda_v^2/\lambda_B^2$. This equation is the stationarity condition for MHD Burgerlence.

In terms of the dimensionless interaction parameters

$$U_1 = \frac{\lambda_v^2 S_v}{6\pi k_{\min}^3 (\nu^t)^3} \quad \text{and} \quad U_2 = \frac{\lambda_B^2 S_B}{6\pi k_{\min}^3 (D^t)^3},$$

the fixed points of Eqs. (40) and (41) are (for $d \sim 1$)

$$\{U_1, U_2\}_a = \left\{ 1 - \sqrt{1-r}, 1 - \frac{2}{r}(1+\sqrt{1-r}) \right\},$$

$$\{U_1, U_2\}_b = \left\{ 1 + \sqrt{1-r}, 1 - \frac{2}{r}(1-\sqrt{1-r}) \right\}, \tag{42}$$

$$\{U_1, U_2\}_c = \left\{ \frac{2}{1+r}, \frac{2r}{1+r} \right\}.$$

The ratio of noise strengths $r \equiv S_B/S_v$ is the only independent parameter. Note that $0 \leqslant r \leqslant \infty$. In particular, r may be greater than 1, implying that the first two solutions may give complex diffusivities. Imaginary components to the transport coefficients suggest the propagation of Alfven waves. The third of Eqs. (42) gives strictly dissipative behavior. Since all three solutions are theoretically possible, the question becomes one of physical accessibility. In other words, given a set of meaningful initial conditions, which asymptotic fixed point will the system approach?

As described above, the hydrodynamic behavior is dominated by the nonlinear terms. These interacting modes were treated mathematically by averaging over spatial scales. A detailed analysis of the scaling behavior, then, will give insight into the asymptotic transport properties of the MHD system. This analysis is provided by the dynamical renormalization group.

3. Renormalization group theory

An alternative method for calculating the scaling exponents is the dynamical renormalization group (RNG). This approach uses the same perturbation series as done previously, but treats the interacting modes differently. Instead of integrating Eqs. (36) and (37) directly, the series is summed successively over small ranges of momenta. This allows differential recursion relations to be derived for the response of the transport coefficients under a scale transformation. The resulting equations give detailed phase flow information on the turbulent diffusivities.

The RNG technique is applied in three steps. First, the series is averaged over an incremental range in momenta. The integrations in Eqs. (36) and (37) are performed over the range $k_{\min} e^{-\delta l} \approx k_{\min}(1-\delta l) \leqslant k \leqslant k_{\min}$ where δl is infinitesimal. To first order (one loop) in the perturbation expansion, the effective transport coefficients are given by

$$\nu^< = \nu + \frac{1}{4\pi}\left[\frac{\lambda_v S_v}{\nu^2} + \frac{\lambda_B S_B}{D^2} \right] \int_{k_{\min}(1-\delta l)}^{k_{\min}} \frac{dk'}{k'^4} \simeq \nu + \frac{1}{4\pi}\left[\frac{\lambda_v^2 S_v}{\nu^2} + \frac{\lambda_B^2 S_B}{D^2} \right] \left(\frac{\delta l}{k_{\min}^3} \right), \tag{43}$$

$$D^< = D + \frac{\lambda_B^2}{2\pi(\nu + D)}\left[\frac{S_v}{\nu} + \frac{S_B}{D} \right] \int_{k_{\min(1-\delta l)}}^{k_{\min}} \frac{dk'}{k'^4} \simeq D + \frac{\lambda_B^2}{2\pi(\nu + D)}\left[\frac{S_v}{\nu} + \frac{S_B}{D} \right] \left(\frac{\delta l}{k_{\min}^{\delta l}} \right), \tag{44}$$

where the superscript t has been replaced by $<$ to emphasize the averaging over the shell of momenta.

These equations now have an effective cutoff $k_{\min} e^{-\delta l}$. The second step returns the system to its original spacing by rescaling the momenta as $k \to k e^{-\delta l}$. This is the same scaling done in Sec. III C 1, with $b = e^{\delta l}$. Using the previous results, the renormalized coefficients are related to $\nu^<$ and $D^<$ by

$$\nu_{\text{renorm}} = \nu + \frac{d\nu}{dl}\delta l = \nu^<[1 + \delta l(a-2)], \tag{45}$$

$$D_{\text{renorm}} = D + \frac{dD}{dl}\delta l = D^<[1 + \delta l(a-2)], \tag{46}$$

To first order in δl, these equations give

$$\frac{d\nu}{dl} = \nu \left[a - 2 + \frac{1}{4\pi\nu k_{\min}^3}\left(\frac{\lambda_v^2 S_v}{\nu^2} + \frac{\lambda_B^2 S_B}{D^2} \right) \right], \tag{47}$$

$$\frac{dD}{dl} = D \left[a - 2 + \frac{1}{2\pi D k_{\min}^3}\left(\frac{\lambda_B^2}{\nu + D} \right)\left(\frac{S_v}{\nu} + \frac{S_B}{D} \right) \right]. \tag{48}$$

There are also similar recursion relations for the coupling coefficients $\{\lambda_v, \lambda_B\}$ and the noise strengths $\{S_v, S_B\}$. Since white noise is invariant to a change of scale, these strengths remain unrenormalized (the more general case is treated in Appendix B). It is shown in Appendix A that there are no corrections to the coupling coefficients (vertices). This is due to the intrinsic Galilean invariance of the original system. As discussed above, this immediately implies the exponent $a = 1$.

The final step of the renormalization group requires that the relevant parameters (i.e., ν and D) remain fixed under the scale transformation. This ensures that the rescaled equations have the same form as the original ones. Setting Eqs. (47) and (48) equal to zero, one sees that the nontrivial fixed

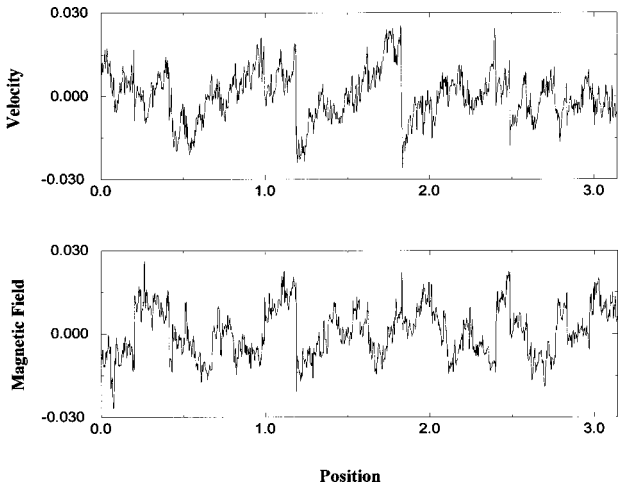

FIG. 3. Velocity and magnetic field of forced MHD Burgerlence as functions of position. The data are plotted on the half-period for clarity.

points are given by Eqs. (38) and (39), except $\{S_v, S_B\} \rightarrow 3\{S_v, S_B\}$. (This discrepancy arises from the different momentum ranges in the two approaches, and would disappear after a full integration of the recursion relations.) With similarly adjusted interaction parameters, the possible branches are given by Eqs. (42).

While the RNG methods give the same scaling behavior as the DIA, as they should, they give more information. In particular, the renormalization group gives the explicit evolution of the transport coefficients under scale transformations. It therefore describes the *approach* to the fixed points in the ν-D phase space.

To analyze this behavior more closely, consider the recursion relations (47) and (48) in terms of the interaction parameters $U_1 = S_v/(2\pi k_{\min}^3 \nu^3)$ and $U_2 = S_B/(2\pi k_{\min}^3 D^3)$:

$$\frac{dU_1}{dl} = 3U_1\left[1 - \frac{1}{2}(U_1 + RU_2)\right], \tag{49}$$

$$\frac{dU_2}{dl} = 3U_2\left[1 - \frac{1}{R}\left(\frac{U_1 + RU_2}{1+R}\right)\right], \tag{50}$$

where $R \equiv (rU_1)/U_2$ and $r = S_B/S_v$ is the ratio of noise strengths. The fixed points of these equations are given by solutions (42). There are two ranges to consider: (1) $r > 1$, giving one real conjugate solution and two complex conjugate solutions; and (2) $r \leqslant 1$, giving three real solutions. Since the recursion relations (49) and (50) are both real, no real initial parameters (U_1, U_2) can evolve to a complex fixed point. In the first regime, then, the third of Eqs. (42) is physically accessible. For $r \leqslant 1$, there is one positive solution and two negative ones for U_2. Figure 4 shows the first quadrant of a phase flow diagram for the representative value $r = \frac{1}{2}$. The arrows indicate the flow under the renormalization transformations (49) and (50). Note in particular that the axes are repellors. Thus, for any physical starting point $(\nu, D) > 0$, only the positive fixed point is accessible. Once again, the third of Eqs. (42) is the infrared limit of the system.

IV. RESULTS AND DISCUSSION

Using the third of Eqs. (42) as the only acceptable solution for the dimensionless interaction parameters, the turbulent transport coefficients are

$$\nu^t = \left[\frac{S_v + S_B}{12\pi}\right]^{1/3} k_{\min}^{-1}, \tag{51}$$

$$D^t = \left[\frac{S_v + S_B}{12\pi}\right]^{1/3} k_{\min}^{-1}. \tag{52}$$

The presence of an infrared divergence suggests an implicit scale dependence as $k^{-1} \sim \sqrt{(\delta x)^2}$. Assuming that $(\delta x)^2 \sim Dt$, this spatial dependence implies that the turbulent motions of the system create ballistic (rather than diffusive) motion, with the speed of propagation given by $[(S_v + S_B)/12\pi]^{1/3}$.

The equality of the transport coefficients reflects a balance between an enhanced fluid transport rate and an increased (and thus more resistant) pressure. From the MHD perspective, the faster magnetic field convection is countered by an enhanced magnetic diffusivity and stronger backreactions. From the gas-dynamic viewpoint, the same nonlinear enhancement of the fluid transport (viscosity) increases the interparticle pressure. In cosmological models, the turbulent pressure (diffusivity) is countered by an enhanced particle ''stickiness.'' The asymptotic state selected is the one that balances the two effects.

Physically, equidissipation results from the twofold action of the nonlinearities: to create shocks through wave steepening and to enhance dissipation. Due to the *N*-wave structure of the velocity shock (see Fig. 2), the dissipation is concentrated within the shock front. Since the only nonlinearity in the induction equation is the vB Lorentz force, magnetic concentrations are triggered by the velocity and localize at the front as well. In this configuration, dissipation occurs almost exclusively within the shock, while the interstitial regions are essentially ideal. The resulting separation provides two mechanical viewpoints for equidissipation:

(1) Using the shock height as a measure of its strength, energy dissipation corresponds to a decrease in height. Heuristically, the ''end points'' must approach each other. However, these end points are shared by the ideal region, where the field is ''frozen in'' to the fluid. Hence, the transport rates must be equal.

(2) A more satisfying view is derived from the equal transport rates of magnetic and fluid energies in the ideal region. Since plasma elements in this region flow into (and out of) the shock, continuity of energy transport requires equal transport coefficients across the shock boundaries. Within the shock, energy transfer may occur, but the receiving field *must* accept energy at the donation rate of the other field.

Thus the equidissipation state results from a dynamic conservation of energy. This is a distinctly separate condition from the *equipartition* of energy. Indeed, a straightforward calculation shows that

$$E_v(k) = |v_k^{(0)}|^2 = \left[\frac{3\pi}{2(S_v + S_B)}\right]^{1/3} S_v k^{-1}, \tag{53}$$

$$E_B(k)=|B_k^{(0)}|^2=\left[\frac{3\pi}{2(S_v+S_B)}\right]^{1/3}S_B k^{-1}. \tag{54}$$

While the vanishing of the magnetic energy with its source is an acceptable limit, the corresponding velocity limit presents an unphysical result for the fluid kinetic energy. Even as $S_v\to 0$, the presence of a mean-square magnetic pressure will cause a transfer of energy to the fluid. The problem is an artifact of expansion (29), where the random forcing was the source of the zero-order velocity field. Since the magnetic pressure is a nonlinear first-order effect, its impact on the fluid energy is not included in Eq. (53). The relevant energy correction is a simple extension of the above calculations, and is given by

$$E_v^1(k)=|v_k^{(1)}|^2=(12\pi)^{1/3}\left[\frac{3}{2}(1-\ln 2)+\frac{5\pi}{\sqrt{3}}\right]S_B^{1/3}k^{-1},$$

with a similar, but always subdominant, correction to the magnetic energy. Equipartition of energy only occurs if $S_v=S_B$, i.e. the forcing strengths must be equal. (This distinction between equal dissipation and energy equipartition has been observed in 3D simulations of incompressible MHD as well [21].) Irrespective of this special case, both energy spectra have the same spatial dependence, a direct result of the conservation of energy. In the more general case of colored noise, this scaling result will hold if the forcing functions themselves have the same spatial dependence. Since the calculations are somewhat more arduous (the noise must now be renormalized as well), we relegate them to Appendix B. The main result is that in an algebraic expansion of the forcing, only spatial powers of the form $S(k)\sim k^{-2\beta}$ will be relevant in the hydrodynamic $(k,\omega\to 0)$ limit. For long-range correlations, these singularities give corresponding energy spectra which scale as $E(k)\sim k^{-1-4\beta/3}$.

These results suggest that the noise sources determine the energy distribution between the fields, while the k dependence of the equidissipation rate controls the turbulent power spectra. The spatial dependence of the effective diffusivities results from the scale similarity of the imposed forcing. Thus, the model of the turbulent steady state is self-consistent and intuitively appealing. Numerical confirmation of this picture is shown in Figs. 5 and 6. Saturation levels for steady-state MHD Burgerlence are shown in Fig. 5. For the ordinary (collisional) transport rates $\nu=2\eta$, the energy levels determined by $S_v=S_B$ and $S_v=2S_B$ are compared. It is clear that equal forcing gives energy equipartition. In addition, the large gap between the saturated energy and bare dissipation indicates the dominance of the turbulent diffusivities. These effective transport rates modify the spectral decay imposed by the forcing. This is shown in Fig. 6 for the cases $S_v\sim S_B\sim k^0$ and $S_v\sim S_B\sim k^{-1}$. Linear fits on the log-log plots give the respective turbulent energy spectra as $\varepsilon_v\sim k^{-1}$ and $\varepsilon_v\sim k^{-5/3}$, in agreement with the analytical predictions.

The explicit form of the energy spectrum represents a competition between the spatial dependence of the forcing and the system's natural tendency to form shocks. This is most clearly apparent for a white-noise source $(S\sim k^0)$, where the presence of forcing at small scales inhibits shock formation, changing the energy spectrum from k^{-2} to k^{-1}. Spatially dependent noise provides an extra parameter, the decay exponent β, for greater modeling freedom. For example, the noise profile $S(k)\sim k^{-1}$ recovers a Kolmogorov spectrum (as found by Chekhlov and Yakhot for the forced Burgers' equation [22]), while $S(k)\sim k^{-3/8}$ generates a KI spectrum. This latter reproduction is particularly interesting, since the KI theory emphasizes the effects of a large-scale field on small-scale energy transfer (the opposite limit considered here). Specifically, a large-scale magnetic field inhibits the cross-field transport of small fluid eddies. In our system, fluid transport is inhibited by small-scale noise and by pressure backreaction. It is the presence of long-range correlations in the applied forcing which allows the model to display the more traditional, inertial-range theories.

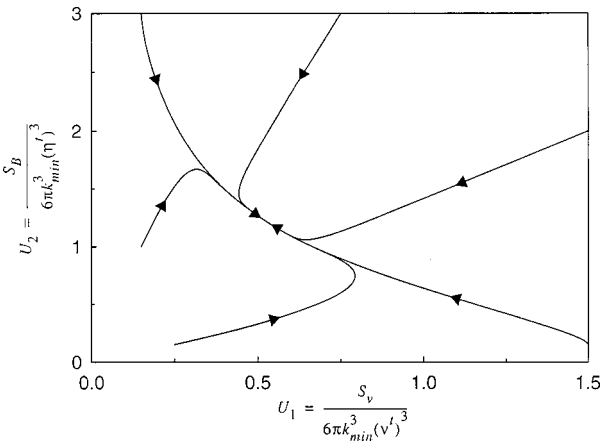

FIG. 4. Renormalization phase flow diagram for the representative value $r\equiv S_B/S_v=\frac{1}{2}$. The trajectories are defined by Eqs. (49) and (50).

V. CONCLUSIONS

We have presented an extension of the Burgers' model of 1D fluid dynamics to include the effects of pressure. When the pressure effects are magnetic, the system represents the simplest possible model of compressible MHD which includes the effects of Alfvenization (the interchange of magnetic and fluid energies). In this case, turbulence is represented by an ensemble of Alfvenic shock waves on a homogeneous density background. Alternatively, the system

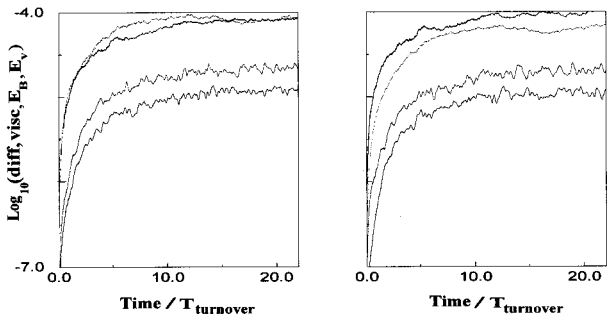

FIG. 5. Saturation levels for steady-state Burgerlence. From the top down, the levels represent the fluid energy, the magnetic energy, viscous damping, and diffusive damping as functions of (normalized) time. (a) Levels for $S_v=S_B$. (b) Levels for $S_v=2S_B$.

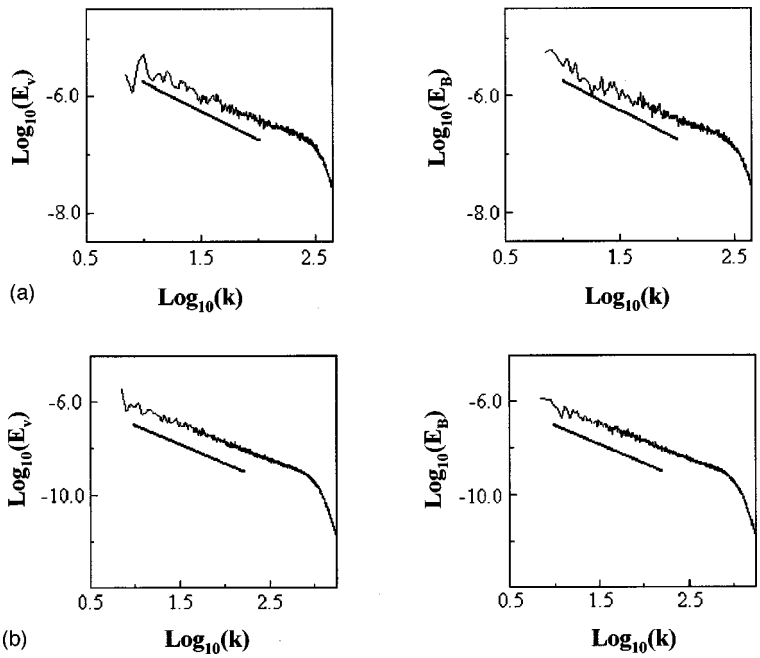

FIG. 6. Representative energy spectra. (a) Energies for $S_v \sim S_B \sim k^0$. The solid line indicates a slope of -1. (b) Energies for $S_v \sim S_B \sim k^{-1}$. The solid line has a slope of $-\frac{5}{3}$. Both of these slopes agree with analytical predictions (see text).

may describe particle gas dynamics, with arbitrary density variations reacting to an adiabatic pressure.

Several dynamical regimes of the system were analyzed. In the limit of unity Prandtl number ($\nu = \eta$), the system decouples into two Burgers' equations in the characteristic variables $v \pm B$. Indeed, since the Hopf-Cole transformation effectively ''matches'' diffusion with ballistic propagation, an exact solution is possible only for the case of equal diffusivities. In the more general case of arbitrary transport coefficients, we applied direct-interaction and renormalization group methods to calculate the turbulent viscosity and diffusivity (i.e, the dynamical decorrelation times) of the randomly forced system. Galilean invariance, obvious in the gas-dynamic interpretation but greatly underappreciated in MHD, simplified the calculations tremendously by precluding vertex (coupling coefficient) renormalizations. It was found that the equidissipation state is the only hydrodynamic ($k, \omega \to 0$) fixed point. Energy equipartition, however, depended on the equality of the forcing functions.

From the viewpoint of self-organization phenomena (e.g., magnetic dynamos, shear-induced mean flow, etc.), this potential disparity in energy levels is rather fortunate. Indeed, it seems unlikely that the energy buildup of one field at the expense of another could happen under the constraint of energy equipartition. A more reasonable scenario is field amplification by equidissipative turbulence, followed by the nonlinear saturation of growth. The system may then relax toward energy equipartition over time.

While this scenario appears to resolve an intrinsic paradox in the Kraichnan-Iroshnikov theory, it relies on a different spectral foundation. In the spirit of Kolmogorov, the KI theory assumes a cascading inertial range free from the large-scale forcing which triggered it. Moreover, the presence of a magnetic field can cause large-scale inhibition of small-scale motion. In contrast, our model assumes a spatially extended noise, with the forcing at small scales creating large-distance effects (e.g., the spreading of wave fronts to prevent shock formation). However, the spatial dependence of the forcing acts an extra parameter, allowing the ''bubbling'' dynamics of our model to effectively mimic an intertial range.

This correspondence suggests that equidissipation is more fundamental to the turbulent state than energy equipartition. While the equality of transport coefficients is certainly robust with regard to random forcing, it would be interesting to see if this equal transport extended beyond the inertial range. In particular, will the system dynamically self-adjust to maintain $\nu + \nu^t = \eta + \eta^t$, regardless of the initial conditions? This would place a fundamental constraint on the onset of intermittency as well. A related concern is the general probability distribution for v and B. The equidissipation state, interpreted as an ensemble of ballistic structures, gives an asymmetric PDF for the characteristic variables $v \pm B$. The distribution before this asymptotic state, and its decoupling into the individual fields, remains an open problem.

APPENDIX A: VERTEX RENORMALIZATION

In order to see how the nonlinear interactions behave under a scale transformation, the perturbation series must be expanded to third-order in the coupling coefficients (vertices) λ_v and λ_B. Equation (27) becomes

$$(-i\omega + \nu k^2) v^{(3)}_{k,\omega} = -ik[\lambda_v (2\langle v^{(0)} v^{(2)} \rangle_{k,\omega} + \langle v^{(1)} v^{(1)} \rangle_{k,\omega}) + \lambda_B (2\langle B^{(0)} B^{(2)} \rangle_{k,\omega} + \langle B^{(1)} B^{(1)} \rangle_{k,\omega})] \tag{A1}$$

where the convolutions

$$\langle XY \rangle_{k,\omega} = \sum_{k',\omega'} X_{k/2-k',\omega/2-\omega'} Y_{k/2+k',\omega/2+\omega'} \tag{A2}$$

are symmetrized for convenience. The factors of 2 arise from the equivalence of $v^{(0)} v^{(2)}$ and $v^{(2)} v^{(0)}$ (and similarly for B) upon integration. Substituting for lower-order terms, such as

$$v^{(1)}_{k/2+k',\omega/2+\omega'} \sim \sum_{k'',\omega''} [\lambda_v v^{(0)}_{k/2+k'',\omega/2+\omega''} v^{(0)}_{k'-k'',\omega'-\omega''} + \lambda_B B^{(0)}_{k/2+k'',\omega/2+\omega''} B^{(0)}_{k'-k'',\omega'-\omega''}] \quad \text{(A3)}$$

gives a Fourier coupling in $\{k,k''\}$, whose effective strength is given by

$$\lambda_v^t = \sum_{k',\omega'} k'^2 \lambda_v^2 \left[\alpha_v(k',\omega') |v^{(0)}_{k',\omega'}|^2 + \left(\frac{\lambda_B}{\lambda_v}\right)^3 \alpha_B(k',\omega') |B^{(0)}_{k',\omega'}|^2 \right], \quad \text{(A4)}$$

$$\lambda_B^t = \sum_{k',\omega'} k'^2 \lambda_B [\beta_v(k',\omega') |v^{(0)}_{k',\omega'}|^2 + \beta_B(k',\omega') |B^{(0)}_{k',\omega'}|^2], \quad \text{(A5)}$$

where

$$\alpha_{\{v,B\}}(k',\omega') = |G_0^{\{v,B\}}(k',gq')|^2 - 2[G_0^{\{v,B\}}(k',\omega')]^2, \quad \text{(A6)}$$

$$\beta_{\{v,B\}}(k',\omega') = \lambda_v |G_0^{\{B,v\}}(k',\omega')|^2 - \lambda_B G_0^v(k',\omega') G_0^B(k',\omega').$$

As before, the bare propagators G_0^v and G_0^B are the linear diffusive Green's functions. Using the continuum approximation $\Sigma_{k',\omega'} \to \int dk' d\omega'/(2\pi)^2$ and performing the integrations (with infrared cutoff $k_{\min}$) gives

$$\lambda_v^t = 0, \quad \text{(A7)}$$

$$\lambda_B^t = \frac{\lambda_B}{6\pi k_{\min}^3 (D+\nu)} \left(\frac{\lambda_v}{\nu} - \frac{\lambda_B}{D}\right)\left(\frac{S_B}{D} - \frac{S_v}{\nu}\right). \quad \text{(A8)}$$

Equation (28) gives an alternative definition for λ_B^t. Expanding to third order, we have

$$(-i\omega + Dk^2) B^{(3)}_{k,\omega} = -ik\lambda_B [\langle v^{(0)} B^{(2)} \rangle_{k,\omega} + \langle v^{(1)} B^{(1)} \rangle_{k,\omega} + \langle v^{(2)} B^{(0)} \rangle_{k,\omega}], \quad \text{(A9)}$$

where the convolutions $\langle \cdots \rangle_{k,\omega}$ are given by Eq. (A2). This equation gives an effective coupling coefficient

$$\lambda_B^t = -\sum_{k',\omega'} k'^2 \lambda_B [M(k',\omega') |v^{(0)}_{k',\omega'}|^2 + N(k',\omega') |B^{(0)}_{k',\omega}|^2], \quad \text{(A10)}$$

where

$$M(k',\omega') = \lambda_B [G_0^B(k',\omega')]^2 + \lambda_v G_0^v(k',\omega') G_0^B(k',\omega') - \lambda_v G_0^v(-k',-\omega') G_0^B(k',\omega'),$$

$$N(k',\omega') = \lambda_v [G_0^v(k',\omega')]^2 + \lambda_v G_0^v(k',\omega') G_0^B(k',\omega') - \lambda_B G_0^v(-k',-\omega') G_0^B(k',\omega'). \quad \text{(A11)}$$

Finally, using the continuum approximation to convert the sum and performing the integrations gives

$$\lambda_B^t = \frac{\lambda_B(\lambda_B - \lambda_v)}{6\pi(D+\nu)^2 k_{\min}^3} \left(\frac{S_B}{D} - \frac{S_v}{\nu}\right). \quad \text{(A12)}$$

Setting $\lambda_v = \lambda_B$ [as done for solutions (22)], this equation determines that $\lambda_B^t = 0$. Since Eq. (A8) must give the same value for λ_B^t, we have $\nu = D$. This is the lower-order result given by straight perturbation theory. Self-consistently iterating this equality in Eq. (A8) would have automatically given $\lambda_B^t = 0$ as well.

APPENDIX B: SPATIALLY DEPENDENT NOISE

To extend the previous results, suppose that the forcing functions are spatially-dependent, so that $S_v = S(k_V)$ and $S_B = S_B(k)$. Under a change of scale, $k \to e^{-\delta l} k$, the noise strengths will rescale as $S(k) \to S(k) - (\delta l) k \partial_k S$. This extra scaling modifies the turbulent transport coefficients and creates nonzero corrections to the forcing (i.e., wave function renormalization). Galilean invariance still ensures that the coupling coefficients remain unchanged.

To examine these changes, we extend the analysis done in Sec. III C 3. In symmetrized form, Eqs. (32) and (33) become

$$(-i\omega + \nu k^2) v^{(2)}_{k,\omega} = -ik \sum_{k',\omega'} [\lambda_v v^{(0)}_{k/2-k',\omega/2-\omega'} v^{(1)}_{k/2+k',\omega/2+\omega'} + \lambda_B B^{(0)}_{k/2-k',\omega/2-\omega'} B^{(1)}_{k/2+k',\omega/2,\omega'}], \quad \text{(B1)}$$

$$(-i\omega + Dk^2) B^{(2)}_{k,\omega} = -ik\lambda_B \sum_{k',\omega'} [v^{(0)}_{k/2-k',\omega/2-\omega'} B^{(1)}_{k/2+k',\omega/2+\omega'} + B^{(0)}_{k/2-k',\omega/2-\omega'} v^{(1)}_{k/2+k',\omega/2+\omega'}], \quad \text{(B2)}$$

where $G_0^v(k,\omega) = (-i\omega + \nu k^2)^{-1}$ and $G_0^B(k,\omega) = (-i\omega + Dk^2)^{-1}$ are the bare propagators.

These equations may also be used to define effective propagators. As before, we can absorb the effects of the new propagators into effective transport coefficients. Consider Eq. (B1) first. For long times ($\omega \to 0$), we have

$$\nu k^2 = \frac{\lambda_v^2}{(2\pi)^2} \int dk' d\omega' \left[\frac{k\left(k' + \frac{k}{2}\right)}{-i\omega' + \nu\left(k' + \frac{k}{2}\right)^2} \right] \times \left[\frac{S_v\left(k' - \frac{k}{2}\right)}{\omega'^2 + \nu^2\left(k' - \frac{k}{2}\right)^4} \right] + \left\{ \begin{matrix} v \to B \\ \nu \to D \end{matrix} \right\}. \quad \text{(B3)}$$

Performing the frequency integral gives

$$\nu k^2 = -\frac{\lambda_v^2}{8\pi\nu^2}\int dk'\left[\frac{k\left(k'+\frac{k}{2}\right)S_v\left(k'-\frac{k}{2}\right)}{\left(k'-\frac{k}{2}\right)^2\left(k'^2+\frac{k^2}{4}\right)}\right]+\left\{\begin{matrix}v\to B\\ \nu\to D\end{matrix}\right\}. \tag{B4}$$

The new propagator contains higher-order terms than the original k^2 of the bare one. Since the hydrodynamic behavior is dominated by the small-k limit, Eq. (B4) may be expanded in powers of k. To lowest order, then, we have

$$\nu k^2 = -\frac{\lambda_v^2}{8\pi\nu^2}\int dk'\left[3S_v(k')-k'\frac{\partial S_v(k')}{\partial k'}\right]\left(\frac{1}{k'^4}\right)+\left\{\begin{matrix}v\to B\\ \nu\to D\end{matrix}\right\}. \tag{B5}$$

To implement the renormalization group, we integrate over the range $k_{\min}e^{-\delta l}\approx k_{\min}(1-\delta l)\leqslant k'\leqslant k_{\min}$, where δl is an infinitesimal change in length. To first order in δl, the turbulent viscosity becomes

$$\nu^t = \frac{\delta l}{8\pi k_{\min}^3}\left[\frac{\lambda_v^2 S_v(k_{\min})}{\nu^2}[3-g_v(k_{\min})]+\frac{\lambda_B^2 S_B(k_{\min})}{D^2}[3-g_B(k_{\min})]\right], \tag{B6}$$

where $g_i(k_{\min})=[k/S_i(k)][\partial S_i(k)/\partial k]|k_{\min}$.

Equation (B2) is evaluated in exactly the same manner, giving an effective diffusivity

$$D^t = \frac{\delta l\lambda_B^2}{2\pi(\nu+D)k_{\min}^3}\left\{\frac{S_v(k_{\min})}{\nu^2}\left[\left(\frac{3}{2}+\frac{\nu-D}{\nu+D}-\frac{g_v(k_{\min})}{2}\right)\right]+\frac{S_B(k_{\min})}{D}\left[\left(\frac{3}{2}-\frac{\nu-D}{\nu+D}-\frac{g_B(k_{\min})}{2}\right)\right]\right\}. \tag{B7}$$

Since the noise is now spatially dependent, it is no longer invariant to a change in scale. The corrections appear explicitly in the autocorrelation functions. For example, first-order velocity perturbations give

$$\langle v_{k,\omega}^{(1)*}v_{k,\omega}^{(1)}\rangle = \sum_{k',\omega'}(k+k')^2|G_0^v(k,\omega)|^2\times[\lambda_v^2|v_{k',\omega'}^{(0)}|^2|v_{k-k',\omega-\omega'}^{(0)}|^2+\lambda_B^2|B_{k',\omega'}^{(0)}|^2|B_{k-k',\omega-\omega'}^{(0)}|^2]. \tag{B8}$$

For long times ($\omega\to 0$), this reduces to

$$\langle v_{k,\omega}^{(1)*}v_{k,\omega}^{(1)}\rangle = \left(\frac{1}{2\pi}\right)^2\int dk'\,d\omega'\left[\frac{(k+k')^2}{\omega'^2+\nu^2k'^4}\right]\times\left[\frac{\lambda_v^2 S_v(k')S_v(k-k')}{\omega'^2+\nu^2(k-k')^2}\right]+\left\{\begin{matrix}v\to B\\ \nu\to D\end{matrix}\right\}. \tag{B9}$$

Performing these integrals, with $k_{\min}(1-\delta l)\leqslant k'\leqslant k_{\min}$, we have

$$S_v^t(k) = \left(\frac{\delta l}{4\pi k_{\min}^3}\right)\left[\frac{\lambda_v^2 S_v^2(k_{\min})}{\nu^3}+\frac{\lambda_B^2 S_B^2(k_{\min})}{D^3}\right]. \tag{B10}$$

Similarly, the noise correction to $S_B(k)$ is obtained from the magnetic autocorrelation $\langle B_{k,\omega}^{(1)*}B_{k,\omega}^{(1)}\rangle$. Using the same procedure, the renormalized noise is

$$S_B^t(k) = \left(\frac{\delta l}{\pi k_{\min}^3}\right)\left[\frac{\lambda_B^2 S_v(k_{\min})S_B(k_{\min})}{\nu D(\nu+D)}\right]. \tag{B11}$$

Using the scalings from Sec. III, we can now write the differential recursion relations of the renormalization group:

$$\frac{d\nu}{dl} = \nu\left[a-2+\left(\frac{\lambda_v^2 S_v(k_{\min})}{8\pi\nu^3 k_{\min}^3}\right)[3-g_v(k_{\min})]+\left(\frac{\lambda_B^2 S_B(k_{\min})}{8\pi\nu D^2 k_{\min}^3}\right)\times[3-g_B(k_{\min})]\right], \tag{B12}$$

$$\frac{dD}{dl} = D\left\{a-2+\frac{\lambda_B^2}{2\pi D(\nu+D)k_{\min}^3}\times\left[\frac{S_v(k_{\min})}{\nu}\left(\frac{3}{2}+\frac{\nu-D}{\nu+D}-\frac{g_v(k_{\min})}{2}\right)+\frac{S_B(k_{\min})}{D}\left(\frac{3}{2}-\frac{\nu-D}{\nu+D}-\frac{g_B(k_{\min})}{2}\right)\right]\right\}, \tag{B13}$$

$$\frac{d\lambda_v}{dl} = \lambda_v[a+c-1]=0, \tag{B14}$$

$$\frac{d\lambda_B}{dl} = \lambda_B[a+c-1]=0, \tag{B15}$$

$$\frac{dS_v(k)}{dl} = S_v(k)[a-2c-1-g_v(k)]+\frac{1}{4\pi k_{\min}^3}\left[\frac{\lambda_v^2 S_v^2(k_{\min})}{\nu^3}+\frac{\lambda_B^2 S_B^2(k_{\min})}{D^3}\right], \tag{B16}$$

$$\frac{dS_B(k)}{dl} = S_B(k)[a-2c-1-g_B(k)]+\frac{1}{\pi k_{\min}^3}\left[\frac{\lambda_B^2 S_v(k_{\min})S_B(k_{\min})}{\nu D(\nu+D)}\right], \tag{B17}$$

Note that for any spatially dependent noise, a cutoff-dependent white noise component is generated. This white-noise correction *does not appear* for uncolored forcing, where scale invariance results in an exact exponent identity. Rather, the extra component is a result of coupled interactions, suggesting that the system responds to spatially correlated forcing by trying to ''balance out'' the discrepancy in scales.

The vertex corrections vanish due to Galilean invariance (see Appendix A), giving the exponent identity $c=1-a$. As before, there is only one independent exponent to find. Setting $d\nu/dl=dD/dl=0$ to obtain the fixed points, Eqs. (B12)

and (B13) give two equations for the exponent a. Consistency then demands that $\nu=D$. Once again, the dissipation rates are equal, even in the case of colored noise.

The exponent a is now expressed in terms of the noise strengths. Plugging this form into Eqs. (B16) and (B17) gives

$$\frac{dS_v(k)}{dl}=3\Bigg(1-\frac{\lambda_v^2 S_v(k_{\min})}{8\pi k_{\min}^3\nu^3}[3-g_v(k_{\min})] - \frac{\lambda_B^2 S_B(k_{\min})}{8\pi k_{\min}^3 D^2\nu}[3-g_B(k_{\min})]\Bigg)S_v(k)-g_v(k)S_v(k) + \frac{1}{4\pi k_{\min}^3}\left[\frac{\lambda_v^2 S_v^2(k_{\min})}{\nu^3}+\frac{\lambda_B^2 S_B^2(k_{\min})}{D^3}\right], \tag{B18}$$

$$\frac{dS_B(k)}{dl}=3\Bigg(1-\frac{\lambda_v^2 S_v(k_{\min})}{8\pi k_{\min}^3\nu^3}[3-g_v(k_{\min})] - \frac{\lambda_B^2 S_B(k_{\min})}{8\pi k_{\min}^3 D^2\nu}[3-g_B(k_{\min})]\Bigg)S_B(k) - g_B(k)S_B(k)+\frac{1}{\pi k_{\min}^3}\left[\frac{\lambda_B^2 S_v(k_{\min})S_B(k_{\min})}{\nu D(\nu+D)}\right]. \tag{B19}$$

If the original noise spectrum had a power-law decay as $k\to 0$, then this behavior would be preserved under rescaling. Moreover, a white-noise component would be generated. Assuming, then, that $S(k)\sim k^{-2\beta}$, the noise spectrum would evolve to $S(k)\to S_0+S_\beta k^{-2\beta}$. For convenience, we consider only the case where the forcing functions have the same k dependence. The recursion relations become

$$\frac{dS_0^v}{dl}=3S_0^v\left[1-\frac{1}{8\pi\nu k_{\min}^3}(\lambda_v^2\mathcal{F}[S_v]+\lambda_B^2\mathcal{F}[S_B])\right] + \frac{1}{4\pi k_{\min}^3}\left[\lambda_v^2\left(\frac{[S_0^v+S_\beta^v k^{-2\beta}]^2}{\nu^3}\right) + \lambda_B^2\left(\frac{[S_0^B+S_\beta^B k^{-2\beta}]^2}{D^3}\right)\right], \tag{B20}$$

$$\frac{dS_0^B}{dl}=3S_0^B\left[1-\frac{1}{8\pi\nu k_{\min}^3}(\lambda_v^2\mathcal{F}[S_v]+\lambda_B^2\mathcal{F}[S_B])\right] + \frac{\lambda_B^2}{\pi k_{\min}^3}\left(\frac{[S_0^v+S_\beta^v k_{\min}^{-2\beta}][S_0^B+S_\beta^B k_{\min}^{-2\beta}]}{\nu D(\nu+D)}\right), \tag{B21}$$

$$\frac{dS_\beta^v}{dl}=S_\beta^v\left[(3+2\beta)-\frac{3}{8\pi\nu k_{\min}^3}(\lambda_v^2\mathcal{F}[S_v]+\lambda_B^2\mathcal{F}[S_B])\right], \tag{B22}$$

$$\frac{dS_\beta^B}{dl}=S_\beta^B\left[(3+2\beta)-\frac{3}{8\pi\nu k_{\min}^3}(\lambda_v^2\mathcal{F}[S_v]+\lambda_B^2\mathcal{F}[S_B])\right], \tag{B23}$$

where

$$\mathcal{F}[S_v]=\frac{3S_0^v+(3+2\beta)S_\beta^v k_{\min}^{-2\beta}}{\nu^2}$$

and

$$\mathcal{F}[S_B]=\frac{3S_0^B+(3+2\beta)S_\beta^B k_{\min}^{-2\beta}}{D^2}.$$

For small values of β, the long-range part of the noise is irrelevant. The (cutoff-dependent) white-noise part dominates, and the above recursion relations reduce to

$$\frac{dS_0}{dl}=3S_0-\frac{9S_0^2}{8\pi k_{\min}^3\nu^3}+\frac{S_0^2}{4\pi k_{\min}^3\nu^3}, \tag{B24}$$

where $S_0=S_0^v+S_0^B$. Here we have let $\nu=D$ for simplicity. The fixed point now gives the effective transport coefficients

$$\nu^t=D^T=\left[\frac{7(S_0^v+S_0^B)}{24\pi}\right]^{1/3}k_{\min}^{-1}. \tag{B25}$$

Using this result, we obtain the scaling exponents $a=\frac{5}{7}$ and $c=\frac{2}{7}$.

From the scaling arguments, the noise transforms as $S\to b^{a-2c-1+2\beta}S$. Hence the long-range part of $S(k)$ takes over if

$$\beta>\beta_c=c+\frac{1-a}{2}=\frac{3}{7}, \tag{B26}$$

leading to new exponents. In this case, the recursion relations become

$$\frac{dS_\beta}{dl}=(3+2\beta)S_\beta\left(1-\frac{3S_\beta}{8\pi k_{\min}^3\nu^3}\right), \tag{B27}$$

where $S_\beta=S_\beta^v+S_\beta^B$. The turbulent diffusivities are now given by

$$\nu^t=D^t=\left[\frac{3(S_\beta^v+S_\beta^B)k_{\min}^{-2\beta}}{8\pi}\right]^{1/3}k_{\min}^{-1}. \tag{B28}$$

For long-range order, then, the scaling exponents are $a=1-2\beta/3$ and $c=2\beta/3$. Higher-order nonlinearities become important (i.e., our system needs more general equations) for $\beta\geqslant\beta_{\max}=\frac{3}{2}$.

With these effective transport coefficients, the energy spectra now become

$$E_v(k)=\left[\frac{\pi}{3(S_\beta^v+S_\beta^B)}\right]^{1/3}S_\beta^v k^{-1-4\beta/3}, \tag{B29}$$

$$E_B(k)=\left[\frac{\pi}{3(S_\beta^v+S_\beta^B)}\right]^{1/3}S_\beta^B k^{-1-4\beta/3}. \tag{B30}$$

Even for colored noise, energy equipartition does not occur unless the forcing functions are equal.

[1] J. Fleischer and P. H. Diamond, Phys. Rev. E **58**, R2709 (1998).
[2] M. Kardar and Y.-C. Zhang, Phys. Rev. Lett. **58**, 2087 (1987).
[3] M. Kardar, G. Parisi, and Y.-C. Zhang, Phys. Rev. Lett. **56**, 889 (1986).
[4] H. van Beijeren, R. Kutner, and H. Spohn, Phys. Rev. Lett. **54**, 2026 (1985).
[5] J. M. Burgers, *The Nonlinear Diffusion Equation* (Reidel, Boston, 1974).
[6] W. Blumen, Geophys. Astrophys. Fluid Dyn. **52**, 89 (1990).
[7] W. Blumen, J. Atmos. Sci. **47**, 2890 (1990).
[8] N. Gurbatov, A. I. Saichev, and S. F. Shandarin, Dokl. Akad. Nauk SSSR **285**, 323 (1985).
[9] F. Shandarin and Ya. B. Zeldovich, Rev. Mod. Phys. **61**, 185 (1989).
[10] D. Montgomery, M. R. Brown, and W. H. Matthaeus, J. Geophys. Res. **92**, 282 (1987).
[11] G. P. Zank and W. H. Matthaeus, J. Geophys. Res. **97**, 17 189 (1992).
[12] J. Friedberg, *Ideal Magnetohydrodynamics* (Plenum, New York, 1987).
[13] D. Forster, D. R. Nelson, and M. J. Stephen, Phys. Rev. A **16**, 732 (1977).
[14] P. G. Saffman, in *Topics in Nonlinear Physics*, edited by L. Sirovich (Springer, Berlin, 1968).
[15] J. M. Thomas, Proc. Am. Math. Soc. **3**, 899 (1952).
[16] R. T. Herbst, Proc. Am. Math. Soc. **7**, 95 (1956).
[17] E. Pinney, Proc. Am. Math. Soc. **1**, 681 (1950).
[18] E. Medina, T. Hwa, M. Kardar, and Y. Zhang, Phys. Rev. A **39**, 3053 (1989).
[19] S. K. Ma, *Modern Theory of Critical Phenomena* (Benjamin, Reading, PA, 1976).
[20] P. H. Diamond and T. S. Hahm, Phys. Plasmas **2**, 3640 (1995).
[21] S. Kida, S. Yanase, and J. Mizushima, Phys. Fluids A **3**, 457 (1991).
[22] A. Chekhlov and V. Yakhot, Phys. Rev. E **51**, R2739 (1995).